MAGNETIC RESONANCE IN MEDICINE 22, 159–166 (1991)

Echo-Planar Time Course MRI of Cat Brain Oxygenation Changes

ROBERT TURNER,*† DENIS LE BIHAN,‡ CHRIT T. W. MOONEN,§
DARYL DESPRES,§ AND JOSEPH FRANK‡

Laboratory of Cardiac Energetics, ‡Diagnostic Radiology Department, and §In Vivo NMR Research Center, National Institutes of Health, Bethesda, Maryland 20892

Received June 25, 1991; revised August 7, 1991

When deoxygenated, blood behaves as an effective susceptibility contrast agent. Changes in brain oxygenation can be monitored using gradient-echo echo-planar imaging. With this technique, difference images also demonstrate that blood oxygenation is increased during periods of recovery from respiratory challenge.

INTRODUCTION

Conventional MR imaging, using only proton density, T1 and T2 contrast, is not sensitive to the rapid but subtle changes in tissue caused by ischemia or hypoxia. Only gross changes in tissue which take hours to appear have been observed in T2-weighted images. Recently Moseley (*1*) and other workers have shown that within 30 min of the onset of ischemia, the diffusion constant of affected brain tissue starts to decrease. Diffusion-weighted images, obtained using the spin-echo sequence developed by Le Bihan (*2*) highlight dramatically the compromised tissue (*3*). Similar changes are seen in the diffusion coefficient of brain tissue within minutes of death (*4, 5*).

The remarkable time resolution of echo-planar imaging (EPI) encourages its use to observe the development of changes in image contrast by means of time course studies. It appears that gradient-echo EPI allows visualization of additional physiological parameters, besides a change in diffusion coefficient. We have used two forms of respiratory challenge, with a duration of 1 min each, in performing EPI gradient-echo imaging of cat brain.

LONG ECHO-TIME GRADIENT-ECHO IMAGING

Gradient-echo imaging is normally used with a very short echo time of a few milliseconds, such as in FLASH or GRASS. As a result, apart from its use in evaluating hematoma (*6*) the potential for visualizing local field inhomogeneities using the gradient-echo method has not yet been fully realized.

If the magnetic susceptibility varies rapidly (in space and/or time) near or within a given voxel, the spins inside experience a range of magnetic fields, and thus precess at varying frequencies. Phase cancellation occurs, and hence a loss of signal, depending on the variation of susceptibility, and the length of time allowed for the spins to precess

† To whom correspondence should be addressed.

0740-3194/91 $3.00

before data acquisition. This of course forms the basis of dynamic susceptibility contrast imaging (*7*), which is producing excellent results in studies of brain perfusion.

The effect has been observed in rat brain at the very high field of 7 T (*8*), where blood vessels become sharply delineated when anesthetic gases are used which reduce blood pO_2. Spin-echo images obtained under identical physiological conditions show no such enhancement. This is nicely explained by the observation that deoxygenated blood is highly paramagnetic (*9, 10*), so that such blood acts as an endogenous intravascular contrast agent, just like Gd-DTPA. Depending on static field strength, the value of T2* for blood increases by more than an order of magnitude between deoxygenated and oxygenated blood (*9*).

Spin-echo and gradient-echo diffusion imaging techniques give consistent values of the diffusion coefficients for live and dead animals, but they differ significantly in the intercepts of the plots of signal versus gradient factor b. In spin-echo imaging the onset of death produces very little change in intercept signal (*11, 12*), while in gradient-echo imaging gray matter intensity changes considerably (Fig. 1) (*13*). The source images were obtained using gradient-echo diffusion EPI (*14, 15*), the postmortem data within 5 min of the lethal injection.

This difference has been tentatively ascribed to the high sensitivity of gradient-echo sequences to the susceptibility changes induced by blood deoxygenation. To confirm this hypothesis, we have used the echo-planar imaging technique to obtain time course studies of brief episodes of anoxia and apnea and of cat brain death. These show striking changes in signal intensity within seconds of the change of oxygenation state of the brain.

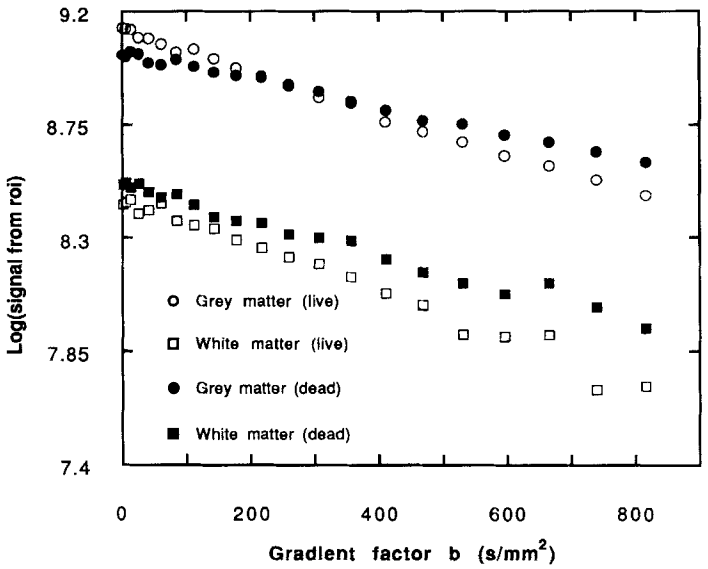

FIG. 1. Plot of ln(signal) versus gradient factor b for selected ROIs in live and dead cat brain (data acquired within 5 min of death). The data were obtained using a gradient-echo echo-planar diffusion imaging sequence. The drop in absolute signal, as well as in slope (diffusion constant) for gray matter upon cat death is evident.

EQUIPMENT AND TECHNIQUE

Images were obtained using a GE 2-T CSI system, equipped with Acustar 290 actively shielded gradient coils, giving a risetime of 200 ms to a maximum gradient of 40 mT m^{-1}. The system software and hardware were upgraded to the Omega configuration during the course of this study; this made no significant differences in the results. A homebuilt 12-cm i.d. birdcage-type rf coil was used.

The MBEST (*16*) gradient-echo echo-planar sequence was employed. The central $(k_x, k_y) = (0, 0)$ echo was formed 45 ms after the initial $\pi/2$ pulse, and the total acquisition time for each 64 × 64 coronal brain image was 82 ms. The in-plane resolution was 1 mm, and the slice thickness was 2 mm. A typical image is shown in Fig. 2.

In general, a high degree of B_0 homogeneity is required to perform EPI imaging; the FID is a better guide than spectral linewidth for obtaining undistorted images of a given slice. Since the gradient-echo does not refocus static field inhomogeneity, the problem is most severe for gradient-echo EPI with long TE.

All animal studies were performed with the approval of the Animal Care and Use Committee of NIH. Three cats were studied, the results for each cat being very similar. Each cat was anesthetized; intubated; ventilated with 1% isoflurane, 30% oxygen, 70%

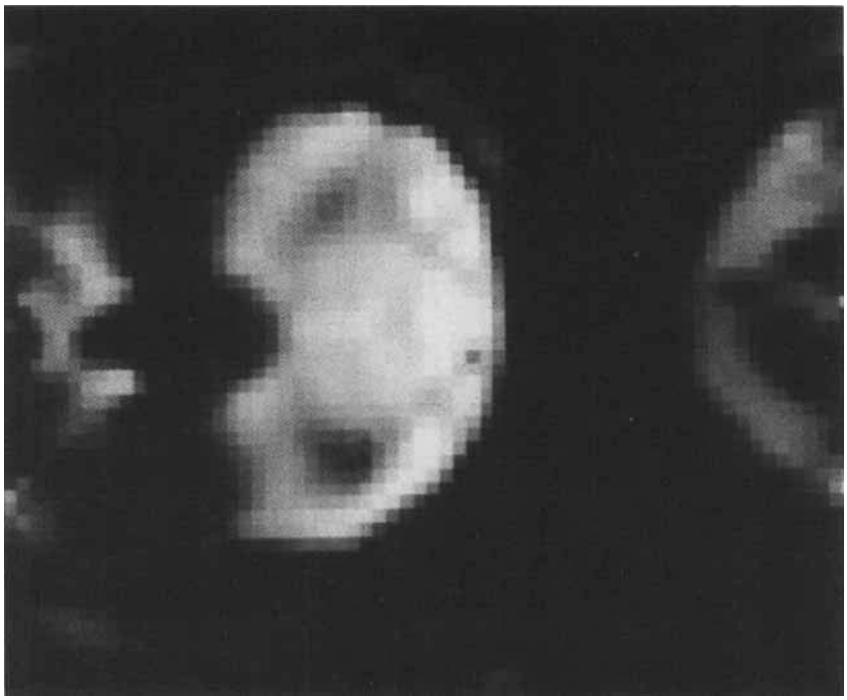

FIG. 2. A typical 64 × 64 gradient-echo EPI cat brain image obtained using a 2.0-T GE Omega CSI system (EPI software written by S. Sukumar and R. Turner). Some wraparound due to the small field of view is visible.

nitrous oxide; and paralyzed with succinylcholine (0.8% solution succinylcholine chloride). Intravenous and intraarterial lines were introduced into the femoral vein and artery. A heating blanket maintained body temperature, blood pressure and core temperature were monitored, and blood gases were periodically checked. The cat's head was held firmly within the rf coil.

When the cat's condition was stable, it was subjected in turn to the following respiratory challenges: (i) Anoxia—respiration for 60 s with pure nitrogen. (ii) Apnea—respiration stopped for 60 s. These were repeated two or three times: neither is likely to cause permanent damage to the CNS. Finally the animal was sacrificed, using either T-61 euthanasia solution or 3 ml KCl, administered intravenously. Blood gases were sampled before, during, and after challenge.

Each of these challenges was initiated 60 s after the beginning of a series of 60 images, obtained at 3-s intervals, so that the respiratory challenge lasted for the middle 20 images of the series. In a similar way, euthanasia was administered 60 s after the beginning of a further series of images.

To facilitate data analysis, difference images were calculated, where the image in each series immediately prior to the onset of respiratory challenge was subtracted from each of the others. "Image" software (written by Wayne Rasband, NIH) running on a Macintosh IIfx computer was used to display images and analyze regions of interest.

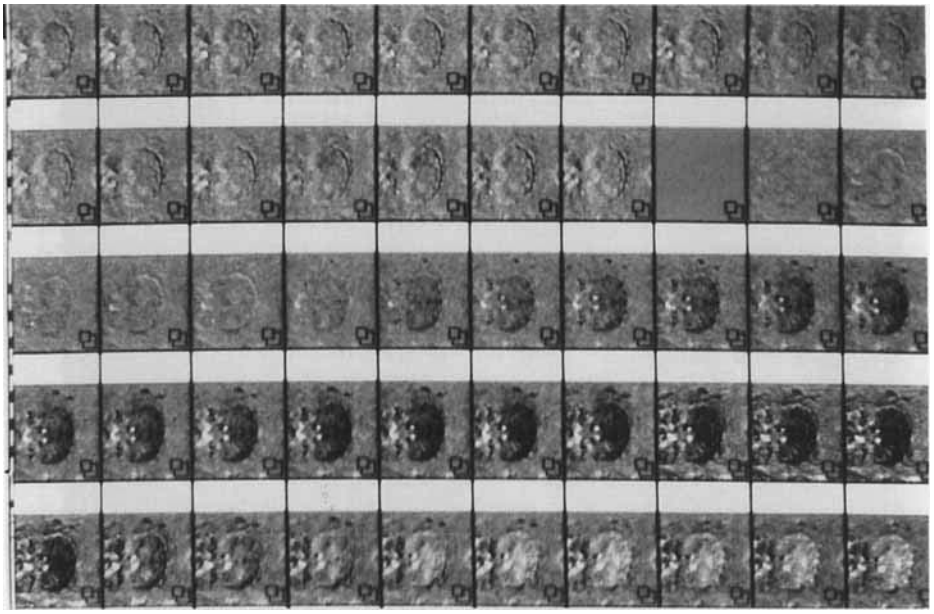

FIG. 3. Array of difference images, spaced 3 s apart. Images are to be read in time sequence from left to right in each line, and from top to bottom. The blank image indicates position of the image subtracted from the remainder of the image series. The breathing gas was changed to pure N_2 at this time. Normal breathing gas was restored 20 images later. Notice the loss of signal during the anoxic period, and the marked overshoot of image brightness during recovery. A small misregistration artifact is visible on the early images, due to a slight movement of cat head when the breathing gas was changed.

RESULTS

The observed changes in contrast are well displayed using arrays of difference images (Figs. 3, 5). Neutral gray represents no change in signal; the "null" image shows in each case the onset of the respiratory challenge. Qualitatively, image brightness indicates the degree of blood oxygenation; darker regions show hypoxemia and brighter regions hyperoxemia.

Figure 3 shows the effect of 1 min of anoxia on image brightness. In this experiment, blood gas measurements showed a drop in pO_2 from 180 to 24 mmHg during the anoxic period, and hemoglobin saturation dropped from 99 to 42%. The rise of intensity following restoration of normal breathing gases is very rapid, taking place in less than 6 s and represents the effect of freshly oxygenated blood entering the brain. The rise time clearly depends on the mean transit time of blood through the brain. Figure 4 shows a graph of the changes in a particular cortical gray matter region of interest. A distinct overshoot can be seen. By 10 min after the anoxic episode, pO_2 was observed to have returned to its normal value.

Figure 5 shows the effect of 1 min of apnea. PO_2 dropped from 185 to 73 mmHg during the period of apnea, while hemoglobin saturation decreased from 99 to 92%. Here the loss of signal during the challenge is quite small, while a noticeable overshoot also occurs when normal breathing is restored. A likely explanation of this observation is that the cat becomes hypercapnic during apnea, and thus the cerebral blood flow is increased. When respiration is restarted the increased blood flow carries surplus oxygen, causing a rise in NMR signal. Figure 6 shows this effect graphically for a gray matter ROI.

Figure 7 demonstrates graphically the loss of signal in gray matter consequent upon cessation of the heartbeat. This drop is very rapid and presumably occurs when the blood loses its oxygen, well before irreversible neuronal damage has taken place.

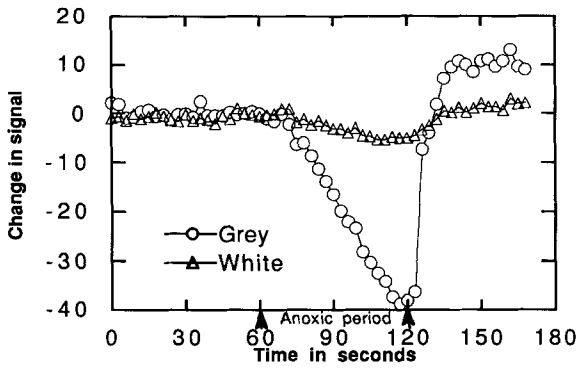

FIG. 4. Plot of the image difference (ROIs in gray and white matter) versus time, for the anoxia experiment. The maximum image intensity was 243. After anoxia commenced the signal for gray matter dropped steadily until oxygen was restored, at which time there was a sudden recovery and overshoot of image intensity. These changes were also seen, though smaller in amplitude, in white matter, reflecting the relative perfusion rates.

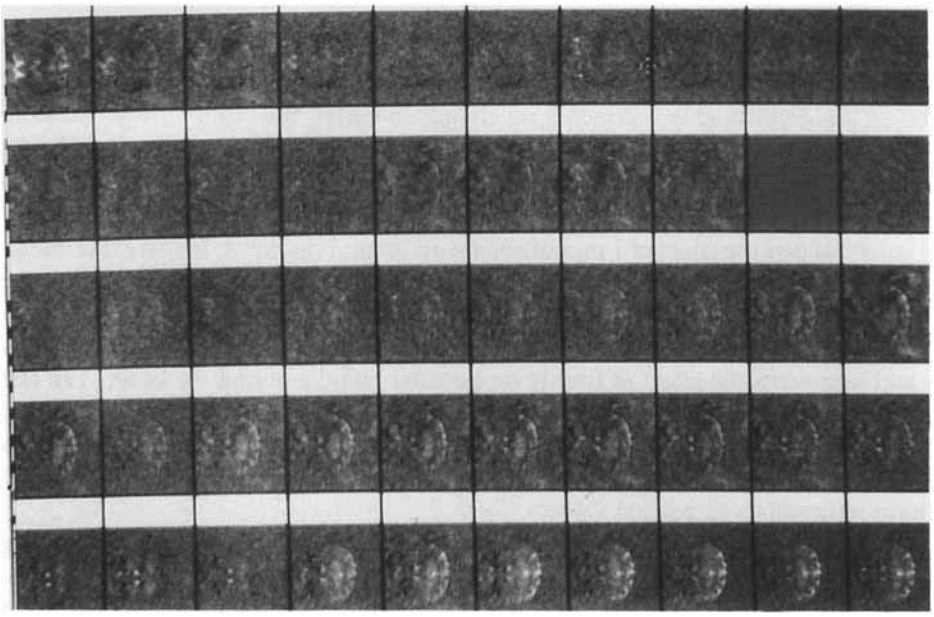

FIG. 5. Array of difference images, spaced 3 s apart. Time sequence of images as in Fig. 3. The blank image indicates position of the image subtracted from the remainder of image series. The ventilator was switched off at this time, and restarted 20 images later. Notice that there was little change in image brightness during apnea, but an increased brightness was seen, consistent with hyperoxemia, when respiration was restarted.

Single pixel signal:noise ratio in the source images was typically 100:1 or better, and results for the three cats studied showed good qualitative consistency. Further experiments are in progress using a larger number of experimental animals.

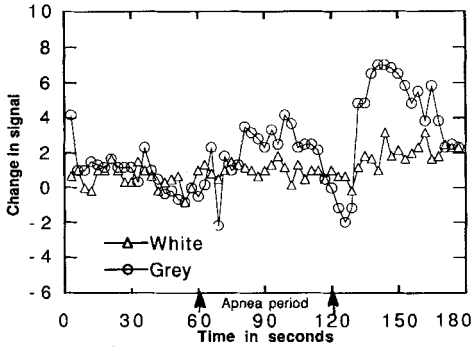

FIG. 6. Plot of image difference (ROIs in gray and white matter) versus time, for the apnea experiment. The maximum image intensity was 241. After ventilation was stopped, the signal for gray matter did not change much until ventilation recommenced, at which time there was a small overshoot of image intensity. SNR does not permit such a change to be seen in white matter.

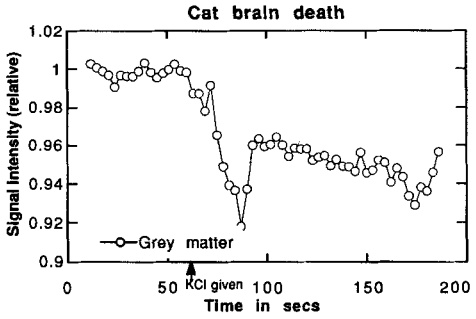

FIG. 7. Plot of image intensity during euthanasia, for a gray matter ROI, versus time. The signal drops sharply when blood flow ceases.

DISCUSSION

The anoxia results shown are consistent with direct local measurements of oxygen pressure (*17*) using a 5% O_2, 95% N_2 respiratory challenge for 1 min in a study of cat cerebral blood flow. These workers found a similar overshoot of blood oxygen following restoration of normal breathing gases. The fact that such an overshoot is manifested in the images as an *increase* of signal intensity during recovery from the challenge demonstrates that the vascular beds responsible for the change in contrast are capillary and/or venous in nature, since at this stage arterial blood is saturated with oxygen, as it was before the challenge. Furthermore, it suggests a transient decoupling between blood flow and oxygen utilization during the first minute of normoxia. It is known that CBF is enhanced during temporary anoxia (*18*), and thus there may be an excess oxygen supply when normoxia is resumed. The depression of metabolism during anoxia, and hence oxygen extraction (*18*), may also persist temporarily after reoxygenation of the blood. The apnea results are consistent with a smaller drop in pO_2 observed in blood gas measurement during the period of apnea. In these preliminary studies, measurements of blood gases were not obtained during the "overshoot" period.

It is not new to observe that deoxygenated blood acts as a paramagnetic contrast agent. However, the ability to monitor noninvasively changes in tissue contrast in real time caused by changes in oxygenation has useful implications. Hyperoxemia and hypoxemia can be visualized directly. In conjunction with flow measurements, and measurements of intravenous pO_2 (*19*), rates of oxygen uptake and loss by cerebral blood may be studied.

Furthermore, the results for apnea suggest that the distribution of cerebral blood flow can be easily visualized, if not quantitated, without the use of an exogenous contrast agent, simply by creating a temporary imbalance between blood flow and oxygen extraction, and imaging rapidly with a gradient-echo technique. The later images in Fig. 3 show clear gray/white matter contrast, purely on the basis of their differential blood flow. Further validation of this totally atraumatic technique could lead to significant improvements in diagnosis and treatment of disease states related to perfusion and oxygen uptake abnormalities, such as hyperacute stroke in humans.

CONCLUSIONS

The use of the long-TE gradient-echo EPI time-course study offers a unique method for observing, in a dramatic way, the effect of rapid changes in blood oxygen levels.

REFERENCES

1. M. E. MOSELEY, J. KUCHARCZYK, J. MINTOROVITCH, Y. COHEN, J. KURHANEWICZ, N. DERUGIN, H. ASGARI, AND D. NORMAN, *Am. J. Neuroradiol.* **11,** 425 (1990).
2. D. LE BIHAN, E. BRETON, D. LALLEMAND, P. GRENIER, E. CABANIS, AND M. LAVAL-JEANTET, *Radiology* **161,** 401 (1986).
3. A. VAN HARREVELD AND S. K. MALHOTRA, *J. Anat.* **101,** 197 (1967).
4. R. TURNER, D. LE BIHAN, C. T. W. MOONEN, AND L. K. HEDGES, *in* "Book of Abstracts, 9th Annual Meeting, Society of Magnetic Resonance in Medicine, 1990," p. 316.
5. J. R. MCFALL, J. H. MAKI, L. HEDLUND, H. BENVENISTE, AND G. COFER. *in* "Syllabus, Workshop on Future Directions in MRI of Diffusion and Microcirculation, Society of Magnetic Resonance in Medicine, 1990," p. 206.
6. R. R. EDELMAN, K. JOHNSON, R. BUXTON *et al. Am. J. Neuroradiol.* **7,** 751 (1986).
7. B. R. ROSEN, J. W. BELLIVEAU, AND D. CHIEN, *Magn. Reson. Q.* **5,** 263 (1989).
8. S. OGAWA, T-M. LEE, A. S. NAYAK, AND P. GLYNN, *Magn. Reson. Med.* **14,** 68 (1990).
9. K. R. THULBORN, J. C. WATERTON, P. M. MATTHEWS, AND G. K. RADDA, *Biochim. Biophys. Acta* **714,** 265 (1982).
10. R. A. BROOKS AND G. DI CHIRO, *Med. Phys.* **14,** 903 (1987).
11. J. R. MCFALL, personal communication.
12. B. R. ROSEN, personal communication.
13. R. TURNER, D. LE BIHAN, J. MAIER, R. VAVREK, L. K. HEDGES, AND J. PEKAR, *Radiology* **177,** 407 (1990).
14. R. TURNER. *GE NMR Instrum. Newslett.* **6,** 4 (1989).
15. R. TURNER AND D. LE BIHAN, *J. Magn. Reson.* **86,** 445 (1990).
16. A. M. HOWSEMAN, M. K. STEHLING, B. CHAPMAN, R. COXON, R. TURNER, R. J. ORDIDGE, M. G. CAWLEY, P. GLOVER, P. MANSFIELD, AND R. E. COUPLAND, *Br. J. Radiol.* **61,** 822 (1988).
17. E. LENIGER-FOLLERT, W. WRABETZ, AND D. W. LÜBBERS, *in* "Oxygen Transport in Tissue-II (J. Grote *et al.,* Eds.), p. 361–367, Plenum, New York.
18. D. BERECZKI, T. OTSUKA, L. WEI, V. R. ACUFF, C. S. PATLAK, AND J. D. FENSTERMACHER, *J. Cereb. Blood Flow. Metab.* **11**(Suppl 2), S72 (1991).
19. K. R. THULBORN, R. M. WEISSKOFF, M. S. COHEN, T. REESE, AND S. R. KIIHNE, *J. Magn. Reson. Imaging* **1,** 149 (1991).